Available online at www.sciencedirect.com

ScienceDirect

Procedia Structural Integrity 18 (2019) 36–45

Structural Integrity Procedia

www.elsevier.com/locate/procedia

25th International Conference on Fracture and Structural Integrity

# Fracture resistance testing of pipeline girth welds with strength undermatch using low-constraint specimens

Claudio Ruggieri[a,*], Diego F. B. Sarzosa[a], Eduardo Hippert Jr.[b]

[a] *Polytechnic School, University of São Paulo, São Paulo 05508-030, Brazil*
[b] *Petrobras Research Center (CENPES), Rio de Janeiro 21941-970, Brazil*

**Abstract**

This work presents an exploratory experimental investigation of the ductile tearing properties for the girth weld of a typical C-Mn pipe internally clad with a nickel-chromium corrosion resistant alloy (CRA) using crack growth resistance curves ($J - \Delta a$ curves). Here, the material of the external pipe is an API 5L Grade X65 pipeline steel whereas the inner clad layer is made of ASTM UNS N06625 Alloy 625 with different mechanical properties. Unloading compliance (UC) testing of the pipeline girth welds employed side-grooved, clamped SE(T) specimens with a weld centerline notch to determine the crack growth resistance curves. This exploratory experimental characterization provides additional toughness data which serve to evaluate the effectiveness of current procedures in determining experimentally measured *R*-curves for dissimilar girth welds.


Peer-review under responsibility of the Gruppo Italiano Frattura (IGF) ExCo.

*Keywords:* Fracture resistance test; *J*-integral; CTOD; unloading compliance method; SE(T) specimen; girth weld; clad line pipe

## 1. Introduction

Structural integrity of submarine risers and flowlines conducting corrosive and aggressive hydrocarbons represents a key factor in operational safety of subsea pipelines. Advances in existing technologies favor the use of C-Mn steel pipelines either clad or mechanically lined with corrosion resistant alloys (CRA), such as ASTM UNS N06625 Alloy 625 (American Society for Testing and Materials, 2009, 2011), for the transport of corrosive fluids. Accurate measurements of fracture resistance properties, including crack growth resistance curves of the girth weld material, become essential in defect assessment procedures of the weldment region and the heat affected zone, where undetected crack-like defects (such as lack of penetration, deep undercuts, root cracks, etc.) may further extend until a critical size is reached. However, while cost effective, fracture assessments of girth welds in lined pipes become more complex due to the dissimilar nature of these materials. A case of interest is represented by deep water steel catenary risers (SCRs) installed by the pipe reeling process which allows pipe welding and inspection to be conducted at onshore facilities. Here, the welded pipe is coiled around a large diameter reel on a vessel and then unreeled, straightened and finally

* Corresponding author. Tel.: +55-11-3091-5184 ; fax: +55-11-3091-5717.
*E-mail address:* claudio.ruggieri@usp.br

2452-3216 
Peer-review under responsibility of the Gruppo Italiano Frattura (IGF) ExCo.
10.1016/j.prostr.2019.08.138

deployed to the sea floor as illustrated in Figs. 1(a-b). While faster and more practical, the reeling process subjects the pipe to large bending load and high tensile forces imposed on the pipeline with a strong impact on stable crack propagation of undetected flaws at girth welds thereby potentially leading to the pipe failure shown in Fig. 1(c) (Garmbis, 2012).


Fig. 1. (a) Reeled pipe lay vessel with a main deck-mounted storage and deployment reel; (b) View of pipe reeling onto the drum; (c) Pipe failure from an undetected flaws at the girth weld (Pictures courtesy of A. Garmbis (2012)).

Engineering critical assessment (ECA) procedures for structural components under ductile regime, including welded structures, rely strongly on crack growth resistance ($J - \Delta a$ or, equivalently, CTOD $-\ \Delta a$) curves (also termed $R$-curves), to characterize crack extension followed by crack instability of the material (Hutchinson, 1983; Anderson, 2005); here, either the $J$-integral or the crack-tip opening displacement (CTOD or $\delta$) describe the intensity of near-tip deformation (Hutchinson, 1983; Anderson, 2005) and $\Delta a$ is the amount of crack growth. These approaches allow the specification of critical crack sizes based on the predicted growth of crack-like defects under service conditions. Current standardization efforts now underway (Shen and Tyson, 2009a,b; Mathias et al., 2013; Cravero and Ruggieri, 2007a,b; Wang et al., 2012; Ruggieri, 2017) advocate the use of single edge notch tension specimens (often termed SE(T) or SENT crack configurations) to measure experimental $R$-curves more applicable to high pressure piping systems, including girth welds of marine steel risers. However, while now utilized effectively in fracture testing of pipeline girth welds with limited overmatch (see, *e.g*, Zhu and McGaughy (2014) and Mathias et al. (2013) for additional details), strong mismatch between the weld metal and base plate strength potentially affects the macroscopic mechanical behavior of the specimen in terms of its load-displacement response with a potentially strong impact on the crack growth resistance curve. Moreover, with the increased use of higher strength pipeline steels, unintended weld strength undermatching emerges as a likely possibility which thus raises strong concerns in integrity assessments of field girth welds produced in lined pipes having circumferential flaws.

This work describes an experimental investigation of the ductile tearing properties for a girth weld of a typical C-Mn pipe internally clad with a nickel-chromium corrosion resistant alloy (CRA) using measured crack growth resistance curves ($J - \Delta a$ curves). Here, the material of the external pipe is an API 5L Grade X65 pipeline steel with

a yield stress of 620 MPa and low hardening properties whereas the inner clad layer is made of ASTM UNS N06625 Alloy 625 with yield stress of 462 MPa and relatively high hardening behavior. Testing of the dissimilar, undermatched girth welds employed side-grooved, clamped SE(T) specimens with a weld centerline notch to determine the crack growth resistance curves based upon the unloading compliance (UC) method using a single specimen technique. This exploratory experimental characterization provides additional toughness data which serve to evaluate the effectiveness of current procedures to measure *R*-curves for this class of material.

## 2. Evaluation Procedure of Fracture Resistance Curve

### *2.1. Experimental Evaluation of the J-Integral*

The $J$-integral for a growing crack can be conveniently evaluated by adopting an incremental procedure which updates its elastic component, $J_e$, and plastic term, $J_p$, at each partial unloading point, denoted $k$, during the measurement of the load *vs*. displacement curve illustrated in Fig. 2(a) in the form

$$J^k = J_e^k + J_p^k \tag{1}$$

where the current elastic term is simply given by

$$J_e^k = \left(\frac{K_I^2}{E'}\right)_k \quad . \tag{2}$$

in which $K_I$ is the elastic stress intensity factor for the cracked configuration, $A_p$ is the plastic area under the load-displacement curve, $B_N$ is the net specimen thickness at the side groove roots ($B_N = B$ if the specimen has no side grooves where $B$ is the specimen gross thickness), $b$ is the uncracked ligament ($b = W - a$ where $W$ is the width of the cracked configuration and $a$ is the crack length), factor $\eta$ represents a nondimensional parameter which relates the plastic contribution to the strain energy for the cracked body and $J$. In writing the first term of Eq.(1), plane-strain conditions are adopted such that $E = E/(1-\nu^2)$ where $E$ and $\nu$ are the (longitudinal) elastic modulus and Poisson's ratio, respectively. We also note that $A_p$ (and consequently, $\eta_J$) can be defined in terms of load-load line displacement (LLD or $\Delta$) data or load-crack mouth opening displacement (CMOD or $V$) data. For definiteness, these quantities are denoted $\eta_{J-LLD}$ and $\eta_{J-CMOD}$.

Since the area under the actual load-displacement curve for a growing crack differs significantly from the corresponding area for a stationary crack which the deformation definition of $J$ is based on (Anderson, 2005; Kanninen and Popelar, 1985) as depicted in Fig. 2(b), the measured load-displacement records must be corrected for crack extension to obtain accurate estimate of $J$-values with increased crack growth. The plastic term, $J_p^k$, can then be evaluated by an incremental formulation proposed by Cravero and Ruggieri (2007b) which is more applicable to crack mouth opening displacement (CMOD) data in the form

$$J_p^k = \left[J_p^{k-1} + \frac{\eta_{J-CMOD}^{k-1}}{b_{k-1}B_N}\left(A_p^k - A_p^{k-1}\right)\right]\cdot\Gamma_k \tag{3}$$

with $\Gamma_k$ defined by

$$\Gamma_k = \left[1 - \frac{\gamma_{LLD}^{k-1}}{b_{k-1}}\left(a_k - a_{k-1}\right)\right] \tag{4}$$

where factor $\gamma_{LLD}$ is evaluated from

$$\gamma_{LLD} = \left[-1 + \eta_{J-LLD}^{k-1} - \left(\frac{b_{k-1}}{W\eta_{J-LLD}^{k-1}}\frac{d\eta_{J-LLD}^{k-1}}{d(a/W)}\right)\right] \tag{5}$$

The incremental expressions for $J_p$ defined by Eqs. (3) to (5) contain two contributions: one is from the plastic work in terms of CMOD and, hence, $\eta_{J-CMOD}$ and the other is due to crack growth correction in terms of LLD by means of $\eta_{J-LLD}$. Thus, evaluation of the above expressions is also relatively straightforward provided the two geometric factors, $\eta_{J-CMOD}$ and $\eta_{J-LLD}$, are known.

### 2.2. Evaluation of Crack Extension

The unloading compliance (UC) technique using a single-specimen test is most commonly employed in current testing protocols to measure the crack growth resistance response in which an estimate of the (current) crack length derives from the specimen compliance measured at periodic unloadings with increased deformation. The slope of the load-displacement curve during the $k$-th unloading depicted in Fig. 2(a) defines the current specimen compliance, denoted $C_k$ ($C_k = V_k/P_k$, where $V_k$ is the current CMOD and $P_k$ represents the current applied load), which depends on specimen geometry and crack length. For the SE(T) crack configurations analyzed here, the specimen compliance based on CMOD is most often defined in terms of a normalized quantity expressed as

$$\mu_{CMOD} = \left[1 + \sqrt{EB_eC_{CMOD}}\right]^{-1} \tag{6}$$

where $\mu_{CMOD}$ defines the normalized compliance for the SE(T) specimen in terms of CMOD. In the above expression, $E$ is the longitudinal elastic modulus, and $B_e$ is the effective thickness defined by

$$B_e = B - \frac{(B - B_N)^2}{B} \tag{7}$$

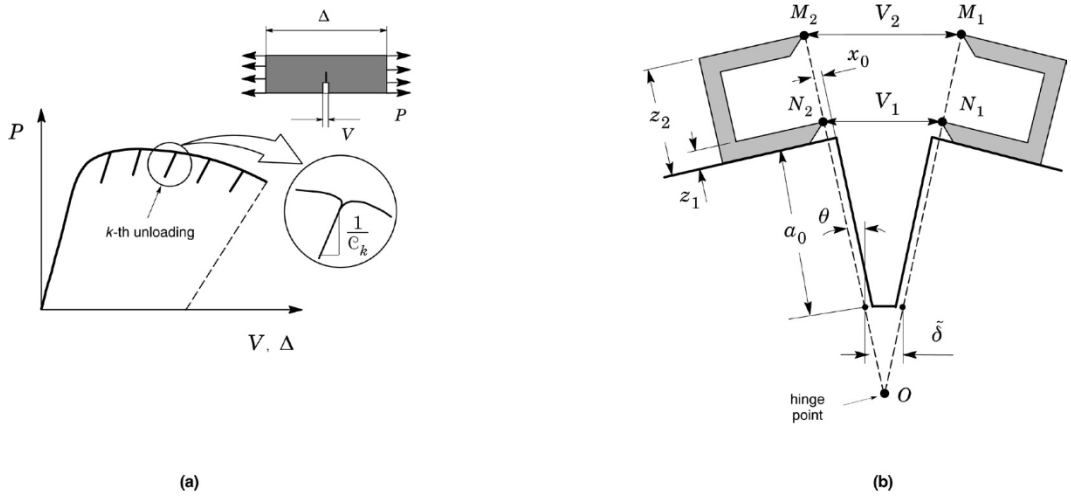


Fig. 2. a) Partial unloading during the evolution of load with displacement. b) Double clip-gage (DCG) method to estimate the CTOD using measurements of crack opening displacements (COD) at two different points.

### 2.3. CTOD Evaluation Procedure

The previous framework also applies when the CTOD is adopted to characterize the crack-tip driving force. The methodology essentially determines the CTOD value from first evaluating the plastic component of $J$ using the plastic work defined by the area under the load vs. CMOD curve and then converting it into the corresponding value of plastic CTOD. The approach has the potential to simplify evaluation of CTOD values while, at the same time, relying on a rigorous energy release rate definition of $J$ for a cracked body yielding the expression (Anderson, 2005; Sarzosa et al., 2015; Kirk and Dodds, 1993; Kirk and Wang, 1995; Zhu and Joyce, 2012)

$$\delta = \frac{J}{m\sigma_0} \tag{8}$$

in which $m$ represents a proportionality coefficient strongly dependent on the material strain hardening but weakly sensitive to crack size as characterized by the $a/W$-ratio. In the above, $\sigma_0$ defines a reference stress value, usually taken as the material yield stress, $\sigma_{ys}$, or the flow stress, $\sigma_f$, defined by $\sigma_f = (\sigma_{uts} + \sigma_{ys})/2$ in which $\sigma_{uts}$ denotes the tensile strength. The choice of $\sigma_0$ has little effect on the absolute value of the CTOD provided a consistent $m$-value is

used in the evaluation procedure. However, $\sigma_f$ is often adopted to make the results less sensitive to the actual strain hardening behavior of the material.

To provide a simpler evaluation procedure for the crack tip opening displacement in SE(T) geometries, a double clip-gage arrangement can also be used as an alternative method to estimate the CTOD from adequate measurements of crack opening displacements (COD) at two different points. Figure 2(b) schematically illustrates the essential features of the procedure in which a pair of knife edges is attached on each side of the notch close to the notch mouth to allow the use of two clip-gages to measure the displacement at these knife edge positions. With the method illustrated in this figure, a simple geometrical approach then enables defining the CTOD ($\delta$) in terms of the two measured COD-values, $V_1$ and $V_2$, at two locations on a straight line passing through the crack flank of the specimen. Thus, by assuming rigid body rotation, the specimen rotation angle yields

$$\sin\theta = \frac{V_1 - \delta}{2(z_1 + a_0)} = \frac{V_2 - V_1}{2(z_2 - z_1)} \tag{9}$$

from which a geometrical relationship between the CTOD ($\delta$) and both measured COD-values is obtained in the form

$$\delta = V_1 - \frac{z_1 + a_0}{z_2 - z_1}(V_2 - V_1) \tag{10}$$

where $z_1$ and $z_2$ represent the distance of the measuring points for $V_1$ and $V_2$ from the specimen surface as depicted in Fig. 2(b). Here, we note that the crack size, $a_0$, entering into Eq. (10) represents the initial crack length not the current crack size measured at the extending tip as discussed by Sarzosa et al. (2015.) Moreover, also observe that the CTOD is defined here as the crack opening at the position of the original crack tip such that, with crack-tip blunting, the position of the original crack tip falls slightly behind the current crack tip.

## 3. Experimental Detais

### *3.1. Material Description and Welding Procedure*

The material utilized in this study was a girth weld of a typical API 5L Grade X65 pipe internally clad with a nickel-chromium corrosion resistant alloy (CRA) made of ASTM UNS N06625 Alloy 625 (American Society for Testing and Materials, 2009, 2011), commercially known as Inconel® 625. The tested weld joint was made from an 8-inch pipe (203 mm outer diameter) having overall thickness, $t_w$ = 19 mm, which includes a clad layer thickness, $t_c$ = 3 mm. Girth welding of the pipe was performed using 100 % $CO_2$ gas-shieded FCAW process in the 5G (horizontal) position with a single V-groove configuration in which the root pass was made by TIG welding in the 2G (vertical) position. The main weld parameters used for preparation of the test weld using the FCAW process are: i) welding current 200 ~ 250 A; ii) welding voltage 27 ~ 29 V; iii) average wire feed speed of 11 ~ 12 m/min.

Table 1 provides the mechanical properties of the base plate material (measured values based on the steel plate certificate) and the weld metal (measured values based on standard tensile testing). Based on Annex F of API 579 (American Petroleum Institute, 2007), the Ramberg-Osgood strain hardening exponents describing the stress-strain response for the base plate and weld metal are estimated as $n_{BM}$ = 18.9 and $n_{WM}$ = 9.7. The measured tensile properties indicate that the weldment undermatches the base plate material by ≈ 25 % at room temperature.

Table 1. Material properties of the base plate and weldment for the tested pipeline CRA girth weld.

| Base Plate | | Weld Metal | |
|---|---|---|---|
| $\sigma_{ys}$ (MPa) | $\sigma_{uts}$ (MPa) | $\sigma_{ys}$ (MPa) | $\sigma_{uts}$ (MPa) |
| 620 | 700 | 462 | 627 |

### 3.2. Clad SE(T) Specimen Geometry

Unloading compliance (UC) tests at room temperature were performed on center notch weld, clamped SE(T) geometries extracted from the longitudinal direction of the pipe specimen to measure tearing resistance properties in terms of $J - \Delta a$ curves. The tested SE(T) specimens have $a/W = 0.3$ and $H/W = 10$ with thickness $B = 16$ mm, width $W = 16$ mm and clamp distance $H = 160$ mm as illustrated in Fig. 3(a). Here, $a$ is the crack depth and $W$ is the specimen width which is slightly smaller than the pipe thickness, $t_w$. Conducted as part of a collaborative program between the University of São Paulo and Petrobras, testing of these specimens focused on the evaluation of crack growth resistance data for nickel-chromium girth welds made in clad lined pipes.

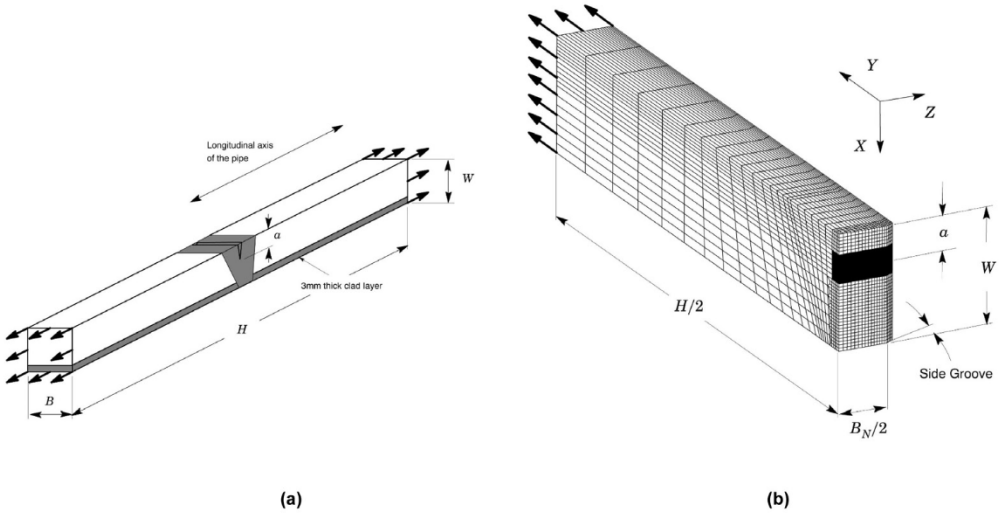


Fig. 3. (a) Geometry of tested weld centerline notched SE(T) specimens with fixed-grip loading extracted from the girth weld of the pipe specimen in the longitudinal direction. (b) Quarter-symmetric 3-D finite element model for the weld centerline notched SE(T) specimens having a clad layer with $a/W = 0.3$.

The specimens were precracked in bending using a three-point bend apparatus very similar to a conventional three-point bend test. After fatigue precracking, the specimens were side-grooved to a net thickness of ~ 85% of the overall thickness (7.5% side-groove on each side) to promote uniform crack growth and tested following some general guidelines described in Ruggieri and Hippert (2015) and ASTM E1820 (American Society for Testing and Materials, 2017). Records of load vs. CMOD were obtained for the specimens using a clip gage mounted on knife edges attached to the specimen surface.

## 4. Compliance and $\eta$-Factor Solutions for the Clad SE(T) Specimen

Because the tested fracture specimens incorporate a clad layer having a relatively strong mismatch in flow properties within the bulk of the specimen (refer to Table 1), application of the framework outlined previously using $\eta$-factors and compliance solutions developed for homogeneous materials may be questioned as it may not accurately describe the specimen response in terms of the evolution of load with CMOD. This section provides the compliance and $\eta$-factor solutions for the tested weld centerline notched SE(T) specimens having a clad layer obtained from detailed 3-D analyses.

Nonlinear finite element analyses are described for 3-D models of SE(T) fracture specimens with fixed clamp distance over specimen width ratio, $H/W = 10$, and cross section dimensions defined by specimen width, $W = B = 16$ mm. The analysis matrix includes 15% side-grooved crack configurations (7.5% side-groove on each side) having

varying crack sizes in the range $a/W = 0.1$ to 0.7 with increments of 0.1 The weld bevel geometry is represented by a V-shaped groove with an included angle of 50º and a root gap of 3 mm - these values characterize well the actual weldment obtained to produce the test specimens. The weld fracture specimen is modeled as a bimaterial component with no transition region such that the mechanical properties for the heat affected zone (HAZ) are not considered. Moreover, a uniform clad layer of thickness, $t_c = 3$ mm, is placed at the bottom of the numerical model as shown in Fig. 3(b). Here, the clad internal layer and the weld metal are considered to have the same mechanical properties as described in Table 1.

Figure 3(b) shows the finite element model constructed for the 3-D analyses of the clamped SE(T) specimen having $a/W = 0.3$. All other crack models for specimens with varying $a/W$-ratios have very similar features. A conventional mesh configuration having a focused ring of elements surrounding the crack front is used with a small key-hole at the crack tip; the radius of the key-hole, $\rho_0$, is 3 $\mu$m (0.003 mm) to enhance computation of $J$-values at low deformation levels. Symmetry conditions permit modeling of only one-quarter of the specimen with appropriate constraints imposed on the symmetry planes. A typical quarter-symmetric, 3-D model has 20 variable thickness layers with $\sim$ 42,000 8-node, 3D elements ($\sim$ 48,000 nodes) defined over the half-thickness ($B/2$); the thickest layer is defined at $Z = 0$ with thinner layers defined near the side groove root region ($Z = 0.425B$) to accommodate strong $Z$ variations in the stress distribution.

Evaluation of the geometric factors, $\eta_{J-CMOD}$ and $\eta_{J-LLD}$, as well as the relationship between $a/W$ and $\mu$ follows from the numerical evolution of load with increased displacement for the numerical models of the clad SE(T) specimens generated by the finite element code WARP3D (Healy et al., 2014). The 3-D solutions for $\eta$-factors incorporating the effects of the clad layer then yield

$$\eta_{J-CMOD} = 1.437 - 3.112\frac{a}{W} + 15.628\left(\frac{a}{W}\right)^2 - 45.767\left(\frac{a}{W}\right)^3 + 58.667\left(\frac{a}{W}\right)^4 - 27.667\left(\frac{a}{W}\right)^5 \tag{11}$$

$$\eta_{J-LLD} = -0.684 + 15.626\frac{a}{W} - 35.142\left(\frac{a}{W}\right)^2 + 2.625\left(\frac{a}{W}\right)^3 + 69.208\left(\frac{a}{W}\right)^4 - 59.001\left(\frac{a}{W}\right)^5 \tag{12}$$

whereas an improved relationship between crack length and normalized compliance is given by

$$a/W = 1.9215 - 13.2195\mu + 58.7080\mu^2 - 155.2823\mu^3 + 207.3987\mu^4 - 107.9176\mu^5 \tag{13}$$

which are valid in the range $0.1 \le a/W \le 0.7$ and it is understood that $\mu \equiv \mu_{CMOD}$

An improved $J - \text{CTOD}$ relationship is also of interest. Evaluation of parameter $m$ entering into Eq. (8) follows from the evolution of $J$ with CTOD for the 3-D numerical models of the weld centerline notched specimens yielding

$$m = 1.932 - 1.845(a/W) + 1.654(a/W)^2 \tag{14}$$

which is also valid in the range $0.1 \le a/W \le 0.7$.

## 5. Crack Growth Resistance Curves

### 5.1. J-Resistance Data

Evaluation of the crack growth resistance curve follows from determining $J$ and $\Delta a$ at each unloading point of the measured load-displacement data. Here, all 3-D expressions for $\eta_{CMOD}$ and $\eta_{LLD}$ s well as the elastic compliance equation developed in previous section are employed to determine the $J$-resistance curves for the tested clad SE(T) specimens

Figure 4 shows the measured crack growth resistance curves in which the overall trend of increased $J$-values with increased amounts of ductile tearing is evident in this plot. Further, observe that, despite some inherent scatter in the measured data, the resistance curves show no sign of leveling off in the entire range of ductile tearing thereby typifying a relatively tough material. Another evident feature in Fig. 4 is the "crack backup" (or apparent negative crack growth) observed in the initial part of the $J - R$ curves for both tested specimens. Such behavior appears to be a recurring feature with this specimen geometry as reported in early works of Joyce et al. (1993) and Joyce and Link

(1995), and more recently by Drexler et al. (2010). While the precise causes of this phenomenon are not yet fully understood, it may be associated with nonstraightness of the crack front after fatigue precracking and large localized deformation at the clamp region early in the test thereby increasing the loading without any measurable increase in CMOD.

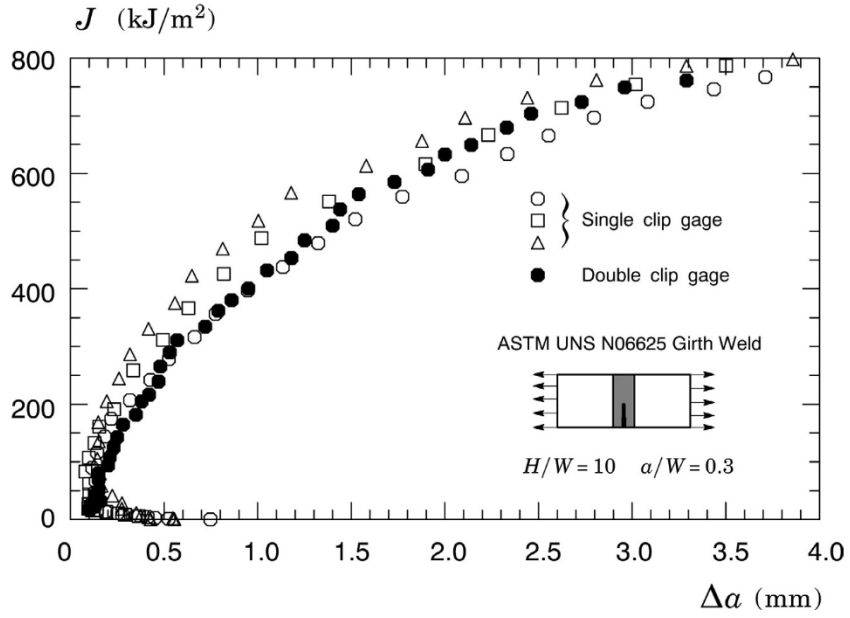


Fig. 4. $J$-resistance curves including crack growth correction for the tested clamped SE(T) specimens based on 3-D $\eta$-factors including the effect of the undermatch weld and clad layer.

### 5.2. CTOD-Resistance Curves

Current defect assessment procedures applicable to piping components, including marine steel catenary risers (SCRs), often adopted by the oil and gas industry favor the use of CTOD–$R$ curves (rather than $J - \Delta a$ data) to define useful toughness values to characterize the material fracture resistance. This section provides crack growth resistance data in terms of CTOD $- \Delta a$ curves in which the crack tip opening displacement derives from the experimentally measured plastic area under the load vs. crack mouth opening displacement (CMOD) curve and from direct measurements using the DCG technique. This study also explores further direct measurements of CTOD obtained from using a digital image correlation (DIC) method.

Figure 5 compares the CTOD $- \Delta a$ curves for the tested girth weld in which the crack tip opening displacement is determined from using three different procedures: 1) CTOD derived from the $J -$ CTOD relationship defined by Eq. (8) with parameter $m$ evaluated by means of Eq. (14) - these $m$-values thus correspond to the 3-D analysis of the weld centerline notched SE(T) specimens having a clad layer; 2) CTOD based on the double clip-gage (DCG) method and 3) CTOD derived from a digital image correlation (DIC) method to determine the relative displacement of the deformed crack flank - here, the CTOD-values during crack growth in the SE(T) specimen are evaluated from placing the measurement points on the flank of the fatigue pre-crack slightly behind the extending crack tip.

This figure shows clearly the effect of different procedures to determine the CTOD-values with increasing crack growth. The DCG-based resistance curve is consistently higher than the CTOD $- \Delta a$ data based on $J$, particularly for larger amounts of stable crack growth, say $\Delta a \gtrsim 1.5$ mm. Here, differences between both methods range from $\sim 25\%$ for $\Delta a = 1.5$ mm to $\sim 45\%$ for $\Delta a = 3$ mm. Observe, however, that the CTOD resistance data based on DCG measurements increase steadily with crack growth for $\Delta a > 1.0$ mm such that the corresponding tearing modulus, which can be simply defined as $d\delta/da$ with CTOD replaced by $\delta$ (Anderson, 2005), remains essentially constant. In contrast, the $J$-based CTOD resistance curves also increase with increased $\Delta a$ but at a much lower rate as characterized

by much smaller values of $d\delta/da$ , particularly at larger amounts of ductile tearing. Moreover, the DIC-based CTOD resistance curve is also closer to the fracture resistance curves obtained by using the $J$ – CTOD relationship. In particular, the DIC-based data agrees well with the CTOD – $R$ curves derived from $J$ for amounts of ductile tearing in the range $\Delta a \leq 2$ mm.

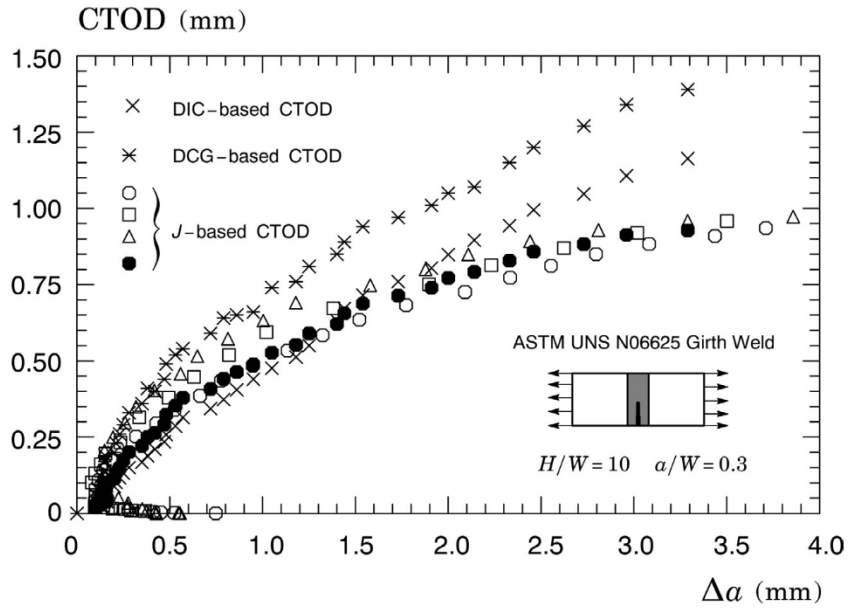


Fig. 5. CTOD-resistance curve derived from measurements of crack opening displacements for the fatigue pre-crack flank using a digital image correlation (DIC) technique.

## 6. Concluding Remarks

This study presents an exploratory experimental investigation of the crack growth resistance properties for the girth weld of an API 5L Grade X65 internally clad with a nickel-chromium corrosion resistant alloy (CRA) of ASTM UNS N06625 Alloy 625. Testing of the pipeline girth welds employed side-grooved, clamped SE(T) specimens with a weld centerline notch to determine the crack growth resistance curves based upon the unloading compliance (UC) method using a single specimen technique. The experiments and fracture resistance data described in this paper show the effectiveness of the UC procedure to characterize ductile tearing properties for dissimilar girth weld materials which serve as a basis for ductile tearing assessments in ECA procedures applicable to clad pipeline girth welds and similar structural components.

A central observation emerging from our work is the rather strong dependence of the CTOD – $R$ curves on the evaluation method of the crack tip opening displacement for the extending crack. In particular, our results show rather convincingly that the CTOD evaluation procedure based on the DCG technique shows a clear tendency to provide higher fracture resistance curves and, consequently, non-conservative fracture assessments. In contrast, DIC measurements of CTOD based on crack flank measurement points provide good agreement with the CTOD – $R$ curve evaluation procedure based on the developed $J$ – CTOD relationship for the clad SE(T) specimen in the range $\Delta a \leq 2$ mm. The analyses and test results described here thus suggest that the use of CTOD – $R$ curves to measure crack growth properties for pipeline girth welds and similar structural components based on $J$ – CTOD relationships may eliminate the potential non-conservatism that would otherwise arise when using DCG-based CTOD – $R$ curves. Clearly, more experimental and analytical studies are needed to clarify the significance of CTOD measurements for growing cracks - this issue appears central to develop a more robust and meaningful CTOD-resistance evaluation procedure.

## Acknowledgements

This investigation is supported by Fundação de Amparo à Pesquisa do Estado de São Paulo (FAPESP) through research grant 2016/26024 – 1. The work of CR is also supported by the Brazilian Council for Scientific and Technological Development (CNPq) through grant 302853/2018 – 9. The authors also acknowledge Petrobras for providing additional support for the work described here and for making available the experimental data.

## References

American Petroleum Institute, 2007. Fitness-for-service, API RP-579-1 / ASME FFS-1.

American Society for Testing and Materials, 2009. Standard specification for Nickel-Chromium-Molybdenum-Columbium alloy (UNS N06625) and Nickel-Chromium-Molybdenum-Silicon alloy (UNS N06219) plate, sheet, and strip, ASTM B443-00.

American Society for Testing and Materials, 2011. Standard specification for Nickel-Chromium-Molybdenum-Columbium alloys (UNS N06625 and UNS N06852) and Nickel-Chromium-Molybdenum-Silicon Alloy (UNS N06219) pipe and tube, ASTM B444-06.

American Society for Testing and Materials, 2017. Standard test method for measurement of fracture toughness, ASTM E1820-17.

Anderson, T.L., 2005. Fracture Mechanics: Fundaments and Applications - 3rd Edition. CRC Press, Boca Raton, FL.

Cravero, S., Ruggieri, C., 2007a. Estimation procedure of $J$-resistance curves for SE(T) fracture specimens using unloading compliance. Engineering Fracture Mechanics 74, 2735–2757.

Cravero, S., Ruggieri, C., 2007b. Further developments in $J$ evaluation procedure for growing cracks based on LLD and CMOD data. International Journal of Fracture 148, 387–400.

Drexler, E., Wang, Y.Y., Sowards, J.W., Dvorak, M.D., 2010. SE(T) testing of pipeline welds, in: 8th International Pipeline Conference (IPC), Calgary, Canada.

Garmbis, A.G., 2012. Engineering Critical Assessment of Submarine Pipelines Subjected to Lateral Loading. MSc Thesis. Polytechnic School, University of So Paulo.

Healy, B., Gullerud, A., Koppenhoefer, K., Roy, A., RoyChowdhury, S., Petti, J., Walters, M., Bichon, B., Cochran, K., Carlyle, A., Sobotka, J., Messner, M., Dodds, R.H., 2014. WARP3D: 3-D Nonlinear Finite Element Analysis of Solids for Fracture and Fatigue Processes. Technical Report. University of Illinois at Urbana-Champaign. http://code.google.com/p/warp3d.

Hutchinson, J.W., 1983. Fundamentals of the phenomenological theory of nonlinear fracture mechanics. Journal of Applied Mechanics 50, 1042–1051.

Joyce, J.A., Hackett, E.M., Roe, C., 1993. Effects of crack depth and mode loading on the $J$-$R$ curve behavior of a high strength steel, in: Underwood, J.H., Schwalbe, K.H., Dodds, R.H. (Eds.), Constraint Effects in Fracture, American Society for Testing and Materials, Philadelphia. pp. 239–263.

Joyce, J.A., Link, R.E., 1995. Effects of constraint on upper shelf fracture toughness, in: Reuter, W.G., Underwood, J.H., Newman, J. (Eds.), Fracture Mechanics, American Society for Testing and Materials, Philadelphia. pp. 142–177.

Kanninen, M.F., Popelar, C.H., 1985. Advanced Fracture Mechanics. Oxford University Press, New York.

Kirk, M.T., Dodds, R.H., 1993. $J$ and CTOD estimation equations for shallow cracks in single edge notch bend specimens. Journal of Testing and Evaluation 21, 228–238.

Kirk, M.T., Wang, Y.Y., 1995. Wide range CTOD estimation formulae for SE(B) specimens, in: Reuter, W.G., Underwood, J.H., Newman, J. (Eds.), Fracture Mechanics, American Society for Testing and Materials, Philadelphia. pp. 126–141.

Mathias, L.L.S., Sarzosa, D.F.B., Ruggieri, C., 2013. Effects of specimen geometry and loading mode on crack growth resistance curves of a high-strength pipeline girth weld. International Journal of Pressure Vessels and Piping 111-112, 106–119.

Ruggieri, C., 2017. Low constraint fracture toughness testing using se(t) and se(b) specimens. International Journal of Pressure Vessels and Piping 156, 23–39.

Ruggieri, C., Hippert, E., 2015. Test Procedure for Fracture Resistance Characterization of Pipeline Steels and Pipeline Girth Welds Using Single-Edge Notched Tension (SENT) Specimens. Technical Report. University of São Paulo.

Sarzosa, D.F.B., Souza, R.F., Ruggieri, C., 2015. $J$-CTOD relations in clamped SE(T) fracture specimens including 3-D stationary and growth analysis. Engineering Fracture Mechanics 147, 331–354.

Shen, G., Tyson, W.R., 2009a. Crack size evaluation using unloading compliance in single-specimen single-edge notched tension fracture toughness testing. Journal of Testing and Evaluation 37, 347–357.

Shen, G., Tyson, W.R., 2009b. Evaluation of CTOD from $J$-integral for SE(T) specimens, in: Pipeline Technology Conference (PTC 2009), Ostend, Belgium.

Wang, E., Zhou, W., Shen, G., Duan, D., 2012. An experimental study on $J$ (CTOD)-$R$ curves of single edge tension specimens for X80 steel, in: 9th International Pipeline Conference (IPC), Calgary, Canada.

Zhu, X.K., Joyce, J.A., 2012. Review of fracture toughness ($G$, $K$, $J$, CTOD, CTOA) testing and standardization. Engineering Fracture Mechanics 86, 1–46.

Zhu, X.K., McGaughy, T., 2014. A review of fracture toughness testing and evaluation using sent specimens, in: 10th International Pipeline Conference (IPC), Calgary, Canada.